ARTICLE

BIOTECHNOLOGY and BIOENGINEERING

Stoichiometric Model and Metabolic Flux Analysis for *Leptospirillum ferrooxidans*

M.P. Merino, B.A. Andrews, J.A. Asenjo

Centre for Biochemical Engineering and Biotechnology, Department of Chemical Engineering and Biotechnology, Millennium Institute for Cell Dynamics and Biotechnology (ICDB): A Centre for Systems Biology, University of Chile, Beauchef 850, Santiago, Chile; telephone: 562-678-4283/4723; fax: 562-699-1084, Chile; e-mail: juasenjo@ing.uchile.cl

Received 18 November 2009; revision received 28 May 2010; accepted 7 June 2010

Published online 29 June 2010 in Wiley Online Library (wileyonlinelibrary.com). DOI 10.1002/bit.22851

ABSTRACT: A metabolic model for *Leptospirillum ferrooxidans* was developed based on the genomic information of an analogous iron oxidizing bacteria and on the pathways of ferrous iron oxidation, nitrogen and CO_2 assimilation based on experimental evidence for *L. ferrooxidans* found in the literature. From this metabolic reconstruction, a stoichiometric model was built, which includes 86 reactions describing the main catabolic and anabolic aspects of its metabolism. The model obtained has 2 degrees of freedom, so two external fluxes were estimated to achieve a determined and observable system. By using the external oxygen consumption rate and the generation flux biomass as input data, a metabolic flux map with a distribution of internal fluxes was obtained. The results obtained were verified with experimental data from the literature, achieving a very good prediction of the metabolic behavior of this bacterium at steady state.

Biotechnol. Bioeng. 2010;107: 696–706.

KEYWORDS: bioleaching; *Leptospirillum ferrooxidans*; iron oxidizing bacteria; metabolic flux analysis; stoichiometric model

Introduction

Bioleaching is the oxidation process of metallic sulfide to soluble metallic ions and sulfuric acid, catalyzed by microorganisms (Schippers and Sand, 1998). The most commonly encountered bacteria in this environment are *Acidihiobacillus ferrooxidans*, *Leptospirillum* sp., *Acidithiobacillus thiooxidans*, and *Acidithiobacillus caldus* (Hallberg and Lindström, 1994; Kelly and Harrison, 1989; Olson et al., 2003; Rohwerder et al., 2003; Schippers and Sand, 1998). The genus *Leptospirillum* is composed of three groups, according to their 16S rRNA phylogeny (Bond and Banfield, 2001): group I represented by *L. ferrooxidans*, group II represented by *L. ferriphilum*, and group III represented by *L. ferrodiazotrophum* (Tyson et al., 2005). *Leptospirillum ferrooxidans* is a Gram-negative chemolithoautotrophic bacterium; it utilizes the energy and reducing power derived from iron oxidation for several metabolic processes, including CO_2 fixation and acquisition of some nitrogen sources (Holmes and Bonnefoy, 2007; Levican et al., 2008; Rawlings, 2005). Assuming a biomass composition represented by $CH_{1.8}O_{0.5}N_{0.2}$ (Jones and Kelly, 1983; Roels, 1983), the stoichiometric equation for biomass formation, obtained for elemental and charge balance can be written in terms of the following reactions (depending on the nitrogen source):

$$CO_2 + \frac{1}{Y_{SX}}Fe^{2+} + 0.2NH_4^+ + \frac{(1-4.2Y_{SX})}{4Y_{SX}}O_2 + \left(\frac{1}{Y_{SX}} - 0.2\right)H^+ \rightarrow CH_{1.8}O_{0.5}N_{0.2} + \frac{1}{Y_{SX}}Fe^{3+} + \left(\frac{1}{2Y_{SX}} - 0.6\right)H_2O \quad (1)$$

$$CO_2 + \frac{1}{Y_{SX}}Fe^{2+} + 0.1N_2 + \frac{(1-4.8Y_{SX})}{4Y_{SX}}O_2 + \frac{1}{Y_{SX}}H^+ \rightarrow CH_{1.8}O_{0.5}N_{0.2} + \frac{1}{Y_{SX}}Fe^{3+} + \left(\frac{1}{2Y_{SX}} - 0.9\right)H_2O \quad (2)$$

In Equations (1) and (2) Y_{sx} represents the biomass yield on ferrous iron (C-mol/mol Fe^{2+}).

Leptospirillum ferrooxidans has been identified as one of the dominant ferrous iron oxidizing microorganisms present in biomining consortia (Rawlings, 1995; Rawlings

Correspondence to: J.A. Asenjo

Contract grant sponsor: Millennium Scientific Initiative
Contract grant number: ICM P05-001-F
Contract grant sponsor: CONICYT
Contract grant sponsor: BioSigma S.A.

et al., 1999), and it plays an important role in bioleaching processes given its ability to attach to sulfide mineral, its high affinity for ferrous iron, and its low sensitivity to inhibition by ferric iron (Norris et al., 1998; Rawlings et al., 1999). Both kinetic studies (Boon et al., 1999b,c; Breed and Hansford, 1999; Breed et al., 1999; Scherpenzeel et al., 1998) and in situ detection methods have demonstrated the importance of *L. ferrooxidans* in these acidic environments rich in iron (Okibe et al., 2003; Schrenk et al., 1998; Tyson et al., 2004).

In this context, *L. ferrooxidans* has become an important objective of biological research, since a better understanding of its metabolic behavior will provide new strategies to improve the productivity of bioleaching process.

A powerful tool for this purpose is metabolic flux analysis (MFA), whereby internal fluxes of a metabolic network are estimated using stoichiometric reaction models for the major intracellular reactions, mass balances for metabolites, and thermodynamics (biochemical reaction directionality; Stephanopoulos et al., 1998, Chapter 8). The set of constraints imposed by the stoichiometry on the distribution of resources through the metabolic network is one aspect of the overall mechanism for cellular control regulation. Therefore, an improved understanding of the stoichiometry is essential for greater understanding of the mechanisms that regulate the cell behavior, and to predict the effect of addition or removal of nutrients or related substances on cell metabolism (Savinell and Palsson, 1992a).

In this work, we investigated the main metabolic pathways of *L. ferrooxidans* with the purpose of developing a stoichiometric model of its catabolism and anabolism. In addition, we performed a MFA to obtain a flux map of the biochemical reactions involved. Such a model will have important applications in seeking conditions to improve practical bioleaching operations. For example, with linear programming (Edwards et al., 2002) it is possible to determine the flux distribution of the cells in a bioleaching tank by optimizing an objective function, such as maximizing growth rate, or minimizing consumption rates of nutrients, like CO_2 (Edwards et al., 2001; Knorr et al., 2007; Oliveira et al., 2005; Schuetz et al., 2007).

Materials and Methods

Metabolic Reconstruction

The whole genome sequence and annotation of *L. ferrooxidans* is not publicly accessible, so a first metabolic reconstruction for this bacterium was done using as reference microorganism *A. ferrooxidans* strain ATCC 23270, whose genome was sequenced by The Institute for Genomic Research (TIGR, www.tigr.org) and Integrated Genomics, Inc. (IG, www.integratedgenomics.com). A metabolic reconstruction of *A. ferrooxidans* is available in MetaCyc (Multiorganism Metabolic Pathways and Enzyme Database, www.metacyc.org), and a stoichiometric model of its central metabolism was recently developed by Hold et al. (2009).

In the present metabolic reconstruction, a manual revision of the enzymes of most conserved pathways was made based on the *A. ferrooxidans* genome annotation. To accept a pathway, the criterion was that the majority of the enzymes (more than 50%) must be present. Likewise, for alternative pathways all the enzymes of each one were sought in the genome annotation for *A. ferrooxidans*, and the one with more identified enzymes was accepted. The information of ferrous iron oxidation, nitrogen fixation, and carbon dioxide assimilation pathways were included, based on experimental evidence for *L. ferrooxidans* found in the literature (Holmes and Bonnefoy, 2007; Parro and Moreno-Paz, 2004; Parro et al., 2007).

In Silico Model Construction and MFA

The stoichiometric model was implemented in the software INSILICO Discovery 1.1. (Stuttgart, Germany, www.insilico-biotechnology.com), which is a computational tool for graphically oriented reconstruction, management and engineering of large-scale cellular networks. With this platform, a graphical representation of the network was obtained, mass and charge balance of the system were checked, and topological and mathematical analysis were performed to determine the internal fluxes of the metabolic network. Finally, a sensitivity analysis of the model was performed according to Nielsen et al. (2003). A random percentage of error in the range of 9–10% over the calculated rates was assumed in different simulations. In order to analyze the sensitivity of the fluxes associated to the experimental error, the resulting flux distributions were compared with the distribution without error.

Theory

By quantifying intracellular fluxes it is possible to analyze nutrient requirements for both anabolic and catabolic processes, and so redesign the culture medium, identify metabolic pathways that limit growth or production, and understand the biochemistry of the cell at a quantitative level. Mathematical modeling and analysis tools like MFA to estimate internal fluxes are of great value for these purposes.

The starting point of MFA is the reaction network describing how substrates are converted into products and biomass. A set of measured extracellular rates are used as input calculations (Stephanopoulos et al., 1998, Chapter 8). The basis of flux determination is a mass balance specified by the stoichiometry of the biochemical network, and the assumption of pseudo-steady state of intracellular metabolites. The general equation that describes the cell metabolism is given by

$$S \cdot v(x) = b \tag{3}$$

where S is the stoichiometric matrix, $v(x)$ holds reaction fluxes in steady state, and b contains experimentally measured exchange rates between the medium and the cell (Savinell and Palsson, 1992b).

The degree of freedom f of this linear system of equations is given by the difference between pathway fluxes and pathway metabolites. So, if exactly f fluxes of $v(x)$ are measured, the system becomes determined, and the solution is unique and simple to obtain. If more than f fluxes are measured, the system becomes over-determined, so extra equations exists that can be used for testing the consistency of the system. If fewer than f fluxes are measured, the system is under-determined and additional inputs are needed to calculate the unknown fluxes (Stephanopoulos et al., 1998, Chapter 8).

Also, an observability test must be applied to the system to establish if the solution could be calculated from the experimentally determined fluxes. It is important to note that a determined or over-determined system is not necessarily observable. If experimental data are redundant, the system as a whole will be not observable. To perform this test, Equation (3) is rearranged by collecting all metabolic substrates, products, and intermediates in the matrix S and rewritten in order to differentiate measured fluxes with calculated fluxes (Nielsen et al., 2003):

$$S_m \cdot v_m + S_c \cdot v_c = 0 \tag{4}$$

Where the subscript m indicates measured rates (in vector v_m) and measurable compounds (in S_m), and c indicates the rates to be calculated in v_c and non-measurable compounds in S_c. Equation (4) can be solved with:

$$v_c = -(S_c^T \cdot S_c)^{-1} \cdot S_c^T \cdot S_m \cdot v_m \tag{5}$$

The system will be observable if the matrix S_c is invertible, so the system can be determined by the relationship:

$$v_c = -S_c^{-1} \cdot S_m \cdot v_m \tag{6}$$

Stoichiometric Model Development

A metabolic reconstruction for *L. ferrooxidans* was performed, including principal pathways of its metabolism. Conserved pathways like central metabolism [Embden–Meyerhof–Parnas (EMP), TCA cycle, pentose phosphate pathway, and anaplerotic reactions], and building blocks biosynthesis pathways (amino acid, nucleotide, and phospholipids) were reconstructed on the basis of the *A. ferrooxidans* genome annotation. Figure 1 show the pathways included in the model.

First Assumptions

In order to obtain a simple but meaningful model, some assumptions were made to decrease its extension without loss of important information:

1. Most of the sequential reactions have been lumped into a single reaction step by eliminating intermediate metabolites that do not participate in other reactions of the network. This process reduces the number of reaction steps without affecting the flux results obtained. It is assumed that lumped reactions proceed at the same rate, and intermediate metabolites are in a steady state.
2. To avoid linear dependences in the stoichiometric matrix, only one cofactor was included in the model. Coenzymes NAD^+/NADH and $NADP^+$/NADPH are interconvertible by the action of the enzyme nicotidamide nucleotide transhydrogenase, so only NAD^+ and NADH were used as substrates for fueling and biosynthetic reactions, respectively (Stephanopoulos et al., 1998).
3. ATP and GTP were pooled together, so we considered ATP/ADP as the only energy transporters. Also, pyrophosphate was interpreted as two single phosphates.
4. Nucleotides, as anabolic building blocks, are represented as monophosphates to avoid phosphorylation/dephosphorylation steps. Therefore, the energy exchange is considered in the polymerization reactions of DNA and RNA.
5. Reversible and irreversible reactions were differentiated in the stoichiometric model, thus, irreversibility constraints were included to solve the system. All the reactions involved in production or consumption of ATP were stated as irreversible in a thermodynamically feasible direction. Moreover, all reactions of assimilation were restricted by the direction of fixation.

Table I lists the stoichiometric equations included in the metabolic model, and Table II shows the nomenclature of its components. A deeper analysis of the pathways is presented in the following section.

Fueling Reactions

Ferrous Oxidation and ATP/NAD(P)H Production

A unifying characteristic of the leptospirilli bacteria is that they are capable of oxidizing ferrous iron as an electron donor to obtain energy for growth and maintenance, using O_2 as electron acceptor (Rawlings, 2002).

The electron transport inside the cell occurs through an enzymatic system composed of a series of cytochromes and quinone pools, being a red cytochrome the initial Fe^{2+} oxidizer (Parro et al., 2007; Tyson et al., 2004). This process

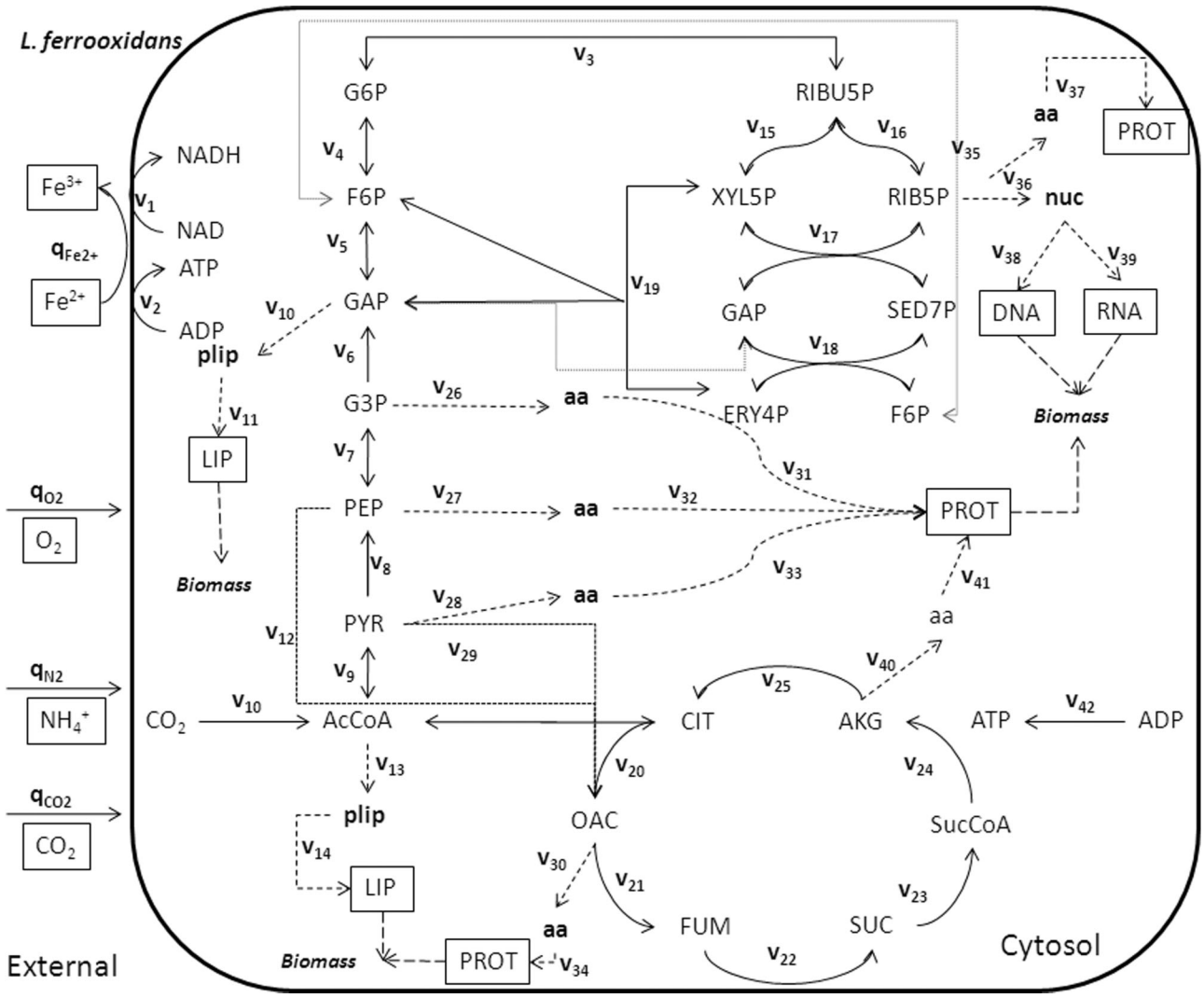

Figure 1. Schematic representation of the main pathways included in the metabolic model of *L. ferrooxidans*. External specific rates are named q_i, and internal flux rates as v_i.

is described by the following equation:

$$2Fe^{2+} + \frac{1}{2}O_2 + 2H^+ \rightarrow 2Fe^{3+} + H_2O \qquad (7)$$

The majority of the protons consumed in the reaction shown in Equation (8) have entered the cell via the ATP synthetase complex embedded in the inner membrane (Holmes and Bonnefoy, 2007). According to White (1995), the synthesis of ATP is coupled to the extrusion of $3H^+$ in iron oxidizing bacteria, as shown in the following equation:

$$3H^+_{EXT} + ADP + Pi \rightarrow ATP + 3H^+_{INT} \qquad (8)$$

Additionally, in Equation (9) the formation of reductive power by the electron transfer from ferrous iron to a NADH ubiquinone, to reduce NAD(P) is included (Ferguson and Ingledew, 2008; Holmes and Bonnefoy, 2007).

$$2Fe^{2+} + NAD(P)^+ \rightarrow 2Fe^{3+} + NAD(P)H \qquad (9)$$

Nitrogen Assimilation

Leptospirillum ferrooxidans is capable of assimilation of nitrogen from different sources. It can either reduce atmospheric N_2 to NH_4^+ using the nitrogenase enzyme complex, or assimilate NH_4^+ from the culture media, which is taken into the cell by ammonia permeases (Norris et al., 1995; Parro and Moreno-Paz, 2004; Parro et al., 2007; Tyson et al., 2004). However, for this analysis it was considered that the nitrogenase complex is inactivated because of its high

Table I. Reactions used in the stoichiometric model of *Leptospirillum ferrooxidans*.

Ferrous oxidation and ATP/NADH production

1. $4FERROUS_{EXT} + 0.5O_2 + NAD + 3H\_IN \Rightarrow 4FERRIC_{EXT} + NADH + H_2O$
2. $3H_{EXT} + ADP + P + H \Rightarrow 3H_{CYT} + ATP + H_2O$

NH_4 assimilation

3. $NH_4 + AKG + NADH + H \Rightarrow GLUT + NAD + H_2O$

CO_2 assimilation

4. $CO_2 + H_2 = FOR + H$
5. $FOR + THF + H = FTHF + H_2O$
6. $SER + THF = GLY + MTHF + H_2O$
7. $FOR + THF + ATP + H + NADH \Rightarrow MTHF + NAD + H_2O + ADP + P$
8. $MTHF + 2FERRH_2 + CO_2 + COA + H_2 \Rightarrow ACCOA + THF + 2FERROX + H_2O + 2H$

Pentose phosphate pathway

9. $G6P + 2NAD + H_2O \Rightarrow RIBU5P + 2NADH + CO_2 + 2H$
10. $RIBU5P = XYL5P$
11. $RIBU5P = RIB5P$
12. $ERY4P + XYL5P = GAP + F6P$
13. $XYL5P + RIB5P = GAP + SED7P$
14. $GAP + SED7P = ERY4P + F6P$

Embden–Meyerhof–Parnas pathway

15. $PYR + ATP + H_2O \Rightarrow PEP + AMP + P + 2H$
16. $PEP + H_2O = G3P$
17. $G3P + ATP + NADH + H \Rightarrow GAP + NAD + P + ADP$
18. $2GAP + H_2O = F6P + P$
19. $F6P = G6P$

TCA cycle

20. $ACCOA + CO_2 + 2FERRH_2 = PYR + 2FERROX + COA + 3H$
21. $FUM + H_2O + NAD \Rightarrow OAC + NADH + H$
22. $SUC + NAD = FUM + NADH + H$
23. $SUCCOA + P + ADP \Rightarrow SUC + COA + ATP$
24. $AKG + NAD + COA \Rightarrow SUCCOA + NADH + CO_2$
25. $CIT + NAD \Rightarrow AKG + NADH + CO_2$
26. $H_2O + OAC + ACCOA \Rightarrow CIT + H + COA$

Anaplerotic reactions

27. $PYR + CO_2 + ATP + H_2O \Rightarrow OAC + ADP + P + 2H$
28. $PEP + CO_2 + H_2O = OAC + P + H$

Amino acid biosynthesis

29. $GLUT + ATP + 2NADH + H \Rightarrow PRO + ADP + 2NAD + P + H_2O$
30. $2ATP + GLUM + CO_2 + 2H_2O \Rightarrow GLUT + 2ADP + P + CARP + 3H$
31. $2GLUT + ACCOA + ASPT + 2ATP + 2H_2O + NADH + CARP \Rightarrow ARGI + FUM + AMP + ADP + COA + NAD + ACET + AKG + 4P + 4H$
32. $OAC + GLUT = ASPT + AKG$
33. $ASPT + ATP + NH_4 + H_2O \Rightarrow ASN + 2P + AMP + H$
34. $ASPT + ATP + 2NADH + 2H + PYR + SUCCOA + GLUT \Rightarrow LYS + ADP + 2NAD + P + COA + AKG + SUC + CO_2$
35. $ASPT + ATP + 2NADH + 2H \Rightarrow HSER + P + 2NAD + ADP$
36. $HSER + ATP + H_2O \Rightarrow THR + ADP + P + H$
37. $THR + PYR + NADH + 2H + GLUT \Rightarrow ILE + NH_4 + CO_2 + NAD + H_2O + AKG$
38. $NH_4 + GLUT + ATP \Rightarrow GLUM + ADP + P$
39. $HSER + ACCOA + NADH + MTHF + HS + H = MET + THF + ACET + COA + NAD$
40. $2PEP + ERY4P + NADH + ATP \Rightarrow CHOR + ADP + NAD + 4P$
41. $CHOR + GLUM + PRPP + SER \Rightarrow TRYP + PYR + GLUT + 2P + H_2O + CO_2 + GAP + 2H$
42. $CHOR + NAD + GLUT \Rightarrow TYR + AKG + NADH + CO_2$
43. $TYR + NAD + H_2O \Rightarrow PHEN + NADH + O_2 + H$
44. $2PYR + NADH + 2H \Rightarrow KIV + NAD + CO_2 + H_2O$
45. $KIV + GLUT = VAL + AKG$
46. $KIV + H_2O + ACCOA + NAD + GLUT \Rightarrow LEU + COA + NADH + H + CO_2 + AKG$
47. $PYR + GLUT = ALA + AKG$
48. $G3P + GLUT + NAD + H_2O \Rightarrow SER + AKG + NADH + P + H$
49. $SER + ACCOA + HS \Rightarrow CYS + COA + ACET$
50. $RIB5P + ATP \Rightarrow PRPP + AMP + H$
51. $PRPP + GLUM + ATP + 2NAD + 5H_2O \Rightarrow HIS + AICAR + AKG + 2NADH + 7H + 5P$

Nucleotide biosynthesis

52. $CARP + ASPT + 1/2O_2 + PRPP \Rightarrow UMP + H_2O + CO_2 + 3P + H$
53. $UMP + NH_4 + ATP = CMP + ADP + P + H$
54. $UMP + 2ATP + 2NADH + H_2O + MTHF \Rightarrow dTMP + 2ADP + 2NAD + 2P + THF$
55. $CMP + NADH + H \Rightarrow dCMP + NAD + H_2O$
56. $PRPP + 2GLUM + GLY + 5ATP + ASPT + FTHF + 4H_2O + CO_2 \Rightarrow AICAR + 5ADP + 7P + 2GLUT + THF + FUM + 9H$
57. $AICAR + FTHF = THF + IMP + H_2O + 2H$
58. $IMP + ASPT + ATP \Rightarrow AMP + ADP + P + FUM + H$
59. $IMP + NAD + 2H_2O + ATP + NH_4 \Rightarrow GMP + AMP + NADH + 2P + 3H$
60. $AMP + NADH + H \Rightarrow dAMP + NAD + H_2O$
61. $GMP + NADH + H \Rightarrow dGMP + NAD + H_2O$

Fatty acid biosynthesis

62. $9ACCOA + 16NADH + 8ATP + H_2O + 8H \Rightarrow C18COA + 8COA + 16NAD + 8ADP + 8P$
63. $8ACCOA + 14NADH + 7ATP + H_2O + 7H \Rightarrow C16COA + 7COA + 14NAD + 7ADP + 7P$
64. $0.5C16COA + 0.5C18COA \Rightarrow C17COA$

Protein biosynthesis

65. $0.096ALA + 0.055ARGI + 0.045ASN + 0.045ASPT + 0.017CYS + 0.049GLUT + 0.049GLUM + 0.115GLY + 0.018HIS + 0.054ILE + 0.084LEU + 0.064LYS + 0.029MET + 0.035PHEN + 0.041PRO + 0.04SER + 0.047THR + 0.011TRYP + 0.079VAL + 0.026TYR + 4.3ATP + 4.3H_2O \Rightarrow PROT + 4.3ADP + 4.3H + 4.3P$

DNA biosynthesis

66. $0.4485DAMP + 0.5515DCMP + 0.5515DGMP + 0.4485DTMP + 6.8ATP + 6.8H_2O \Rightarrow DNA + 6.8ADP + 6.8P + 6.8H$

RNA biosynthesis

67. $0.27575CMP + 0.27575GMP + 0.22425AMP + 0.22425UMP + 2ATP + 2H_2O \Rightarrow RNA + 2ADP + 2P + 2H$

Lipid biosynthesis

68. $GAP + NADH + H \Rightarrow GLYC3P + NAD$
69. $GLYC3P + 2C17COA + ATP + H_2O \Rightarrow DIAGLYC + 2COA + 2P$
70. $DIAGLYC + GLYC3P + H_2O \Rightarrow PGLYC + AMP + P$
71. $PGLYC \Rightarrow 0.5GLYC + 0.5CLIPIN$
72. $DIAGLYC + SER \Rightarrow PETH + CO_2 + AMP$
73. $0.762PETH + 0.143PGLYC + 0.095CLIPIN \Rightarrow LIP$

Carbohydrate biosynthesis

74. $G6P + ATP + H_2O \Rightarrow CARBOH + ADP + H$

Acetyl CoA synthetase

75. $ACET + COA + ATP + H_2O = ACCOA + AMP + 2P + H$

Glycerol synthesis

76. $GAP + NADH + H + H_2O = GLYC + NAD + P$

ATP maintenance

77. $ATP + H_2O \Rightarrow ADP + P + H$

Assimilative reduction of SO_4

78. SO_4 $ATP + 4NADH + 2H \Rightarrow HS + 4NAD + ADP + AMP + 3P + H_2O$

Biomass formation

79. $0.03DNA + 0.16RNA + 0.52PROT + 0.17CARBOH + 0.09LIP \Rightarrow BIO$

Extracellular transport

80. $NH_{4EXT} + 4ATP + 4H_2O \Rightarrow NH_{4CYT} + 4ADP + 4P + 4H$
81. $CO_{2EXT} = CO_{2CYT}$
82. $H_2O_{EXT} = H_2O_{CYT}$
83. $O_{2EXT} = O_{2CYT}$
84. $G6P_{EXT} = G6P_{CYT}$

Table I. (*Continued*)

85. $SO_{4EXT} + ATP + H_2O \Rightarrow SO_{4CYT} + ADP + P + H$
86. $P_{EXT} + ATP + H_2O \Rightarrow P_{CYT} + ADP + P + H$
87. $H_{2EXT} = H_{2CYT}$

Irreversible reactions are indicated with an arrow ($\Rightarrow$), and reversible reactions with an equal ($=$).

sensitivity to oxygen, and the elevated energy requirements that implies. Therefore, ammonia is assimilated by the GDH pathway (reaction 10), assuming no ammonia limitation in the culture media (Kanamori et al., 1987).

$$NH_4^+ + AKG + NAD(P)H + H^+ \rightarrow GLUT + NAD(P)^+ + H_20 \quad (10)$$

CO_2 Assimilation

According to Parro et al. (2007), *L. ferrooxidans* assimilates CO_2 through the reductive acetyl-CoA pathway, where one CO_2 is captured by a special tetrahydrofolate cofactor and reduced to a methyl group (reactions 4–7 in Table I). The other CO_2 is reduced to a carbonyl group by the enzyme CO dehydrogenase, which is then combined with the methyl group to form acetyl-CoA by a collection of enzymes called the acetyl-CoA synthetase complex (reaction 8, Table I). This pathway seems to require hydrogen gas as the electron donor and it is very efficient, requiring only $4H_2$ per acetate formed (Hügler et al., 2003; Menon and Ragsdale, 1999). ATP and NAD(P)H required for this process are obtained from ferrous iron oxidation.

Synthesis of Precursor Metabolites

Pentose Phosphate Pathway (PPP)

Oxidative and non-oxidative branches of this pathway were included in the stoichiometric model. According to the simplification criterion described previously, the oxidative branch was reduced to a single reaction (reaction 9), and all reactions of the non-oxidative branch were incorporated into the model (reactions 10–14).

Embden–Meyerhof–Parnas Pathway (EMP)

Several chemolithoautotrophic microorganisms are capable of operating their central carbohydrates metabolism in anabolic and catabolic directions in order to achieve long- and short-term adaptation. An important regulation point of this pathway is the PEP/pyruvate interconversion reaction (Tjaden et al., 2006).

In chemolithoautotrophic iron/sulphur oxidizing bacteria, like *L. ferriphilum*, *A. ferrooxidans*, and *A. thiooxidans*, it has been demonstrated that genes of phosphoenolpyruvate synthetase, which catalyzes the conversion of pyruvate to PEP, are present. However, the genes of the reverse reaction, catalyzed by the enzyme pyruvate kinase, have been identified only in *A. ferrooxidans* and *A. thiooxidans*. Furthermore, genes of phosphoenolpyruvate diquinase, which catalyzes this reaction in a bidirectional way, were also missing in *L. ferriphilum* (Levican et al., 2008). Therefore, the EMP pathway in *Leptospirillum* probably works preferentially in an anabolic direction, so this pathway was included with these directional restrictions (reactions 15–19).

TCA Cycle

Although the TCA cycle in *L. ferriphilum* runs in a reductive manner to fix CO_2 (Levican et al., 2008), it was incorporated into the model in an oxidative direction (reactions 20–26) because it is thought that *L. ferrooxidans* fixes CO_2 through an acetyl-CoA reductive pathway.

Anaplerotic Reactions

In order to keep a constant level of intermediary metabolites of the TCA cycle, to maintain metabolic balance in the cell, two anaplerotic reactions were included in the stoichiometric model, catalyzed by the enzymes pyruvate carboxylase and phosphoenolpyruvate carboxylase (reactions 27 and 28). Other anaplerotic reactions have not been included to avoid the introduction of reaction cycles, which could lead to observability problems in the mathematical analysis.

Biosynthesis of Building Blocks

Amino Acid Biosynthesis

Amino acid biosynthesis reactions were classified into five families, according to the specific precursor metabolite or amino acid that serves as the starting point for their synthesis (Stephanopoulos et al., 1998, Chapter 2, p. 60). The reactions included are considered as standard reactions, so no further analysis will be incorporated (reactions 29–51, Table I).

Nucleotide Biosynthesis

Standard pathways of pyrimidine and purine nucleotides biosynthesis were incorporated into the stoichiometric model (reactions 52–61). All nucleotides were expressed as monophosphates, assuming that their activation to triphosphates is carried out on polymerization reactions to RNA and DNA.

Fatty Acid Biosynthesis

It was assumed that *L. ferrooxidans* only synthesized fatty acids as building blocks for its cell membrane phospholipids

Table II. Nomenclature of components included in the metabolic model of *Leptospirillum ferrooxidans*.

Abbreviation	Name
ACCOA	Acetyl-CoA
ACET	Acetate
ADP	Adenosine diphosphate
AICAR	5′-Phosphoribosyl-5-amino-4-imidazolecarboxamide
AKG	Alpha-ketoglutarate
ALA	L-Alanine
AMP	Adenosine monophosphate
ARGI	Arginine
ASN	L-Asparagine
ASPT	Aspartate
ATP	Adenosine triphosphate
BIO	Biomass
C16COA	Palmitic acid CoA
C17COA	Synthetic fatty acid
C18COA	Steric acid CoA
CARBOH	Carbohydrates
CARP	Carbamoyl phosphate
CHOR	Chorismate
CIT	Citrate
CLIPIN	Cardiolipin
CMP	Cytidine-3′-monophosphate
CO_2	Carbon dioxide
COA	Coenzyme A
CYS	L-Cysteine
dAMP	2′-Deoxyadenosine 5′-monophosphate
dCMP	2′-Deoxycytidine 5′-monophosphate
dGMP	2′-Deoxyguanosine 5′-monophosphate
DIAGLYC	CDP-diacylglycerol
DNA	Deoxyribonucleic acid base pair
dTMP	Deoxythymidine 5′-monophosphate
ERY4P	D-Erythrose 4-phosphate
F6P	Fructose-6-phosphate
$FERRH_2$	Reduced ferredoxin
FERRIC	Ferric iron
FERROUS	Ferrous iron
FERROX	Oxidized ferredoxin
FOR	Formate
FTHF	Formyl tetrahydrofolate
FUM	Fumarate
G3P	Glycerate 3-phosphate
G6P	Glucose-6-phosphate
GAP	Glyceraldehyde 3-phosphate
GLUM	L-Glutamine
GLUT	L-Glutamate
GLY	L-Glycine
GLYC3P	Glycerol 3-phosphate
GLYC	Glycerol
GMP	Guanosine 5′-monophosphate
H_2	Hydrogen
H_2O	Water
H	Proton
H_IN	Internal proton
H_OUT	External proton
HIS	L-Histidine
HS	Sulfide
HSER	L-Homoserine
ILE	Isoleucine
IMP	Inosine monophosphate
KIV	2-Keto-isovalerate
LEU	L-Leucine
LIP	Synthetic lipid molecule
LYS	L-Lysine
MET	L-Methionine
MTHF	5,10-Methylene tetrahydrofolate
N_2	Nitrogen
NAD	Nicotinamide adenine dinucleotide (oxidized)
NADH	Nicotinamide adenine dinucleotide (reduced)
NH_4	Ammonia ion
O_2	Oxygen
OAC	Oxaloacetate
P	Orthophosphate
PEP	Phosphoenolpyruvate
PETH	Phosphatidylethanolamine
PGLYC	Phosphatidyl glycerol
PHEN	L-Phenylalanine
PRO	L-Proline
PROT	Protein
PRPP	5-Phosphoribosyl-1-pyrophosphate
PYR	Pyruvate
RIB5P	D-Ribose 5-phosphate
RIBU5P	D-Ribulose 5-phosphate
RNA	Ribonucleic acid nucleotide
SED7P	Sedoheptulose 7-phosphate
SER	L-Serine
SO_4	Sulphate
SUC	Succinate
SUCCOA	Succinyl-CoA
THF	Tetrahydrofolate
THR	L-Threonine
TRYP	L-Tryptophan
TYR	L-Tyrosine
UMP	Uridine 5′-monohosphate
VAL	L-Valine
XYL5P	D-Xylulose 5-phosphate

(Hold et al., 2009). As the composition of fatty acid and their length is unknown for *L. ferrooxidans*, for simplicity, a synthetic-theoretical fatty acid, called C17-CoA was considered, composed of equal proportions of the major fatty acids in bacteria, C16:0 and C18:0 (Hold et al., 2009; Stephanopoulos et al., 1998) represented in reactions 62–64.

Synthesis of Macromolecules

Protein Biosynthesis

Protein synthesis reactions were obtained assuming an analogous composition of amino acids to *E. coli*. Therefore, the protein was considered as a polypeptide of standard composition, which requires 4.3 ATP for the correct addition of one amino acid to the existing protein (reaction 65) (Hold et al., 2009; Stephanopoulos et al., 1998, Chapter 2, p. 68).

DNA Biosynthesis

As reported by Sand et al. (1992), the G+C content of *L. ferrooxidans* fluctuates in the range of 53.9% and 56.4%.

Thus, for the stoichiometric model we assumed an average composition of 55.2% of dGMP and dCMP and 44.8% of dAMP and dTMP per base pair. Also, it was considered that 2 ATPs were consumed per nucleotide incorporated as the total energetic cost of unwinding the double helix before DNA replication, 4 ATP to activate monophosphates to triphosphates, and 0.8 ATPs for proofreading (Stephanopoulos et al., 1998, Chapter 2, pp. 69–70). Hence, the energy requirements for 1 bp formation are 6.8 ATPs. Consequently reaction 66 represents the elongation of the DNA chain by 1 bp.

RNA Biosynthesis

RNA composition was approximated by values from DNA (Hold et al., 2009), so GMP and CMP constitutions were set at 27.6%, and 22.4% for AMP and UMP. As stated by Ingraham et al. (1983), the energetic cost for the incorporation of one ribonucleotide as monophosphate is 0.4 ATP. Also, as mentioned before, 2 ATPs are required to activate monophosphate to triphosphates, hence 2.4 ATPs are required to synthesize one nucleotide of RNA (reaction 67).

Lipid Biosynthesis

As mentioned above, it was assumed that *L. ferrooxidans* only synthesizes membrane-forming phospholipids, because the production of energy storage molecules on this bacterium is unknown (Hold et al., 2009). Thus, a general phospholipid was created, composed of a 76.2% phosphatidylethanolamine, 14.3% phosphatidylglycerol, and 9.5% cardiolipin (Stephanopoulos et al., 1998, Chapter 2, p. 64) (reactions 68–73).

Carbohydrate Biosynthesis

Carbohydrates are defined as molecules with an approximate stoichiometric formula $C_n(H_2O)_m$ and they mainly play a role in three aspects: as part of the cell wall (murein), as energy storing molecules and finally as metabolites. A general carbohydrate was built as is shown in reaction 74.

Results and Discussion

Stoichiometric Model

The in silico metabolic network of *L. ferrooxidans* was constructed from database and literature information from an analogous iron oxidizing bacteria (See Materials and Methods Section for detail). When an incomplete pathway arises, the principal criterion to approve it was that more than 50% of the enzymes involved must be present. Thus, standard pathways, for example, biosynthesis of amino acid phenylalanine, lysine, methionine, and alanine were incomplete; however, iron oxidizing bacteria like *A. ferrooxidans* and *L. ferrooxidans* must contain these pathways because they are capable of growth in basal medium 9K (Silverman and Lundgren, 1959). Nevertheless, the opposite case is also possible, but further biochemical confirmation, through enzymatic activity assays, for example, is necessary to complete the pathway validation.

A simplification process was performed in order to reduce the complexity of the stoichiometric model. With the purpose of reducing the number of metabolites and reactions, sequential reactions were grouped in one net reaction in conserved pathways, like the EMP, the pentose phosphate and the amino acid biosynthesis pathways. Also linearly dependent reactions were eliminated to avoid observability problems of the model. That is the case of the anaplerotic reactions of pyruvate carboxylase and the glyoxylate shunt, which when included together, make the system non-observable since the latter is a linear combination of the pyruvate carboxylase reaction and the TCA cycle. Hence, the glyoxylate shunt was considered to be inactive in our simulations, assuming that the corresponding enzymes operate under different environmental conditions.

The metabolic model developed includes the main sources for catabolic and anabolic processes of *L. ferrooxidans*. The main catabolic substrates considered are ferrous iron, as energy source in aerobic conditions and CO_2 from the air as sole carbon source. Also, nitrogen assimilation was assumed to occur from NH_4^+ as the unique source. In addition, the main anabolic final products considered are the macromolecules DNA, RNA, protein, carbohydrates, and lipids constituting one C-mol of biomass according to reaction 79 in Table I. A schematic representation of the reconstructed metabolic network is shown in Figure 1.

The model has 86 reactions, where 10 of them are transport reactions of nutrients and products (reactions 1, 2, and 80–87). It is composed of 100 metabolites, of which 88 are intermediate metabolites, and must be balanced. Consequently, the resulting system has 2 degrees of freedom, thus two external fluxes must be estimated to achieve a determined system and so calculate the internal fluxes of Figure 1.

Proof of Concept

In order to prove the functionality and feasibility of the metabolic model developed, a proof of concept was made. For this purpose, two external fluxes were estimated from published data. The calculation of the internal fluxes was made assuming a specific growth rate of *L. ferrooxidans* on ferrous iron $\mu = 0.05$ (h^{-1}) (Boon, 1996; Kleerebezem and Loosdrecht, 2008). A specific oxygen consumption rate was estimated through a relationship between this and the dilution rate in continuous culture taken from Scherpenzeel et al. (1998):

$$q_{O_2} = \frac{D}{0.047} + 0.057 \qquad (11)$$

Table III. Assumed percentage of each macromolecule (x_i) in cell composition of *L. ferrooxidans* (taken from Stephanopoulos et al., 1998, Chapter 2, p. 75 for *E. coli*).

Macromolecule	x_i (g/g_{cdw})
Protein	0.52
DNA	0.03
RNA	0.16
Lipids	0.09
Carbohydrates	0.17

A value of $q_{0_2} = 1.12$ (mol O_2/C-mol h^{-1}) was obtained for $D = 0.05$ (h^{-1}) (equal to the specific growth rate μ for a steady-state continuous culture).

The biomass generation at $D = 0.05$ (h^{-1}) was obtained using the biomass composition in Table III.

In order to obtain a determined and observable system, the estimated specific oxygen consumption rate and the generation rate of biomass were used as input data for the MFA, considering a standard deviation of 10%. With this analysis, a flux distribution was obtained, which is shown in Figure 2.

In Figure 2, it is possible to observe a scheme of the contribution of the different pathways to the global metabolic process. It can be seen that the TCA cycle is running in a reductive manner, which is very reasonable, because it would be inefficient for *L. ferrooxidans* to use the regular TCA cycle releasing the CO_2 needed for growth. This behavior is consistent with that observed for *Leptospirillum ferriphilum* by Levican et al. (2008).

Main uptake fluxes predicted with MFA are shown in Table IV.

The growth yield on ferrous iron was calculated with the equation

$$Y_{SX} = -\frac{\mu}{q_S} \tag{12}$$

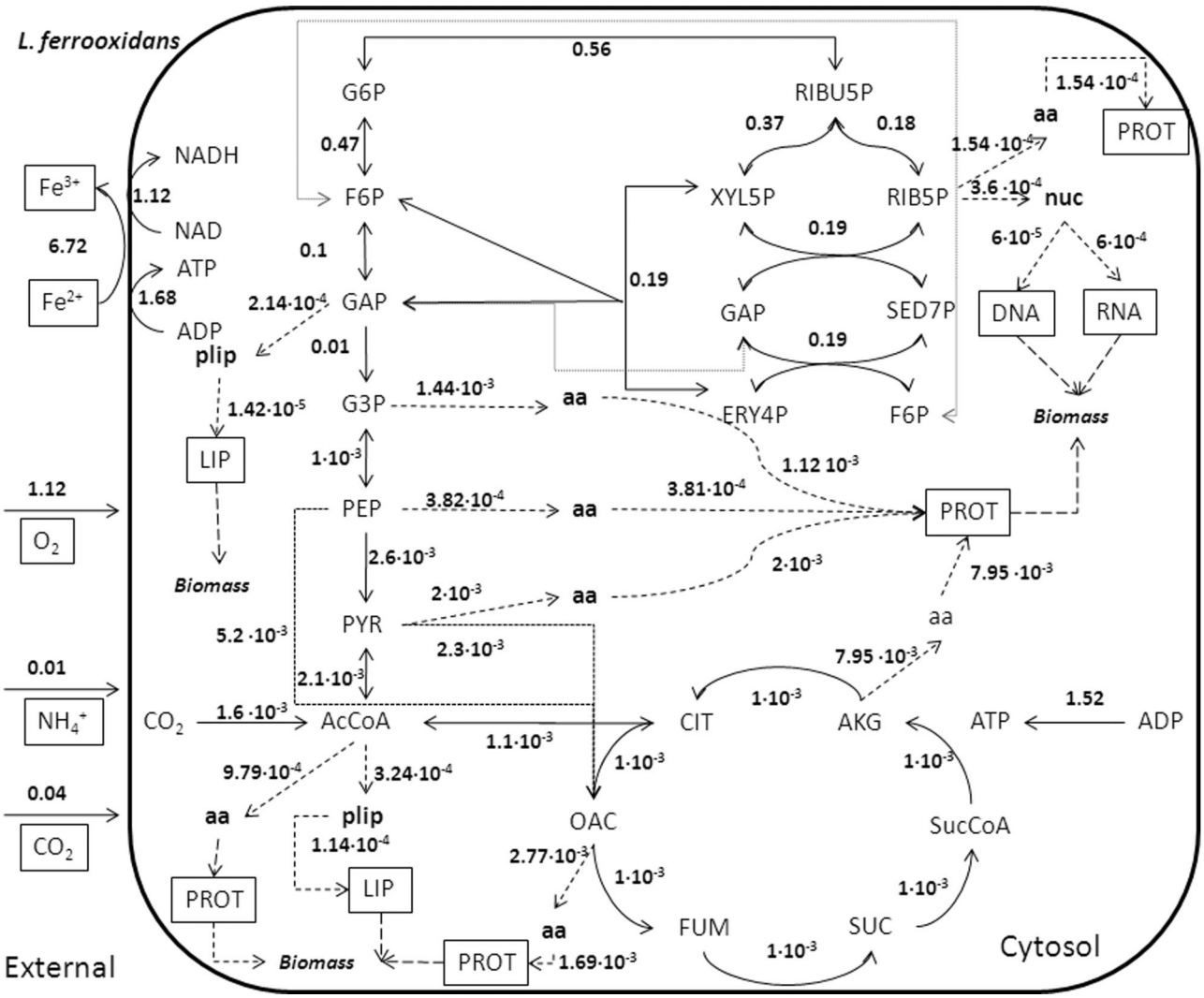

Figure 2. Metabolic flux distribution of *L. ferrooxidans* in (mol/C-mol h^{-1} of biomass).

Table IV. Calculated uptake specific rates with MFA for *L. ferrooxidans* using NH_4^+.

Calculated flux value	mol/C-mol h^{-1}
qCO_2	0.04
qNH_4^+	0.01
qFe^{2+}	6.72
qATP	1.68

Consequently, a yield of *L. ferrooxidans* on ferrous iron of $Y_{SX} = 0.007$ (C-mol/mol Fe^{2+}) was obtained, which compared with $Y_{SX} = 0.006$ (C-mol/mol Fe^{2+}) for *L. ferrooxidans* in Breed et al. (1999), $Y_{SX} = 0.010$ (C-mol/mol Fe^{2+}) for *Leptospirillum* sp. by Scherpenzeel et al. (1998), and $Y_{SX} = 0.006$ (for iron oxidizing bacteria) by Mignone and Donati (2004), indicating a very good prediction of the model for this iron oxidizing bacteria growing on ferrous iron.

A sensitivity analysis was done using a random percentage of error in the range of 9–10% of the input data. Three simulations were carried out considering different measurement errors, and the flux distribution obtained in each case was very stable since the direction of the fluxes remains equal to the original distribution, and the calculated rates reveal only slight variations.

The elimination of the anaplerotic reactions catalyzed by the enzymes pyruvate carboxylase and phosphoenolpyruvate carboxylase was explored, determining that the elimination of any of these enzymes makes impossible the biomass generation by the metabolic network. The activity of both enzymes is necessary because they are the only way to generate oxaloacetate, which is required in biomass biosynthesis.

A simulation was made activating the nitrogenase enzyme to compare the flux distribution in the presence and absence of this pathway. When the enzyme is activated one degree of freedom is added to the metabolic system, so three external fluxes are needed to solve it. Considering a specific growth rate of $\mu = 0.05$ (h^{-1}), and the stoichiometric coefficients of Equation (2), a specific nitrogen consumption rate of $q_{N_2} = 0.005$ (mol N_2/C-mol h^{-1}) was calculated. Thus, the input data is the same as in the other condition, but including a nitrogen reduction rate. With this test, we observed that the model predicts that the nitrogenase reaction runs in the opposite direction, which indicates that *L. ferrooxidans* cannot use this nitrogen source for growth under the stated conditions, because of the high-energetic requirements.

Conclusions

A description of the main metabolic pathways of *L. ferrooxidans* was made. The principal uptake pathways considered in the metabolic reconstruction were ferrous iron oxidation to gain energy for all anabolic and catabolic processes, CO_2 assimilation through the acetyl-CoA reductive pathway, and ammonia assimilation by the GDH pathway. A stoichiometric model composed of 86 reactions and 2 degrees of freedom was obtained. The model was used to calculate the internal flux distribution by MFA. With these data, an estimation of growth yields of *L. ferrooxidans* on ferrous iron was made, obtaining $Y_{SX} = 0.006$ (C-mol/mol Fe^{2+}), showing a very good behavior when compared with experimental data from the literature. A sensitivity analysis was performed, and the model shows a very stable behavior when a random error on the input data is considered. In conclusion, the metabolic model developed is capable of reproducing the main aspects of the metabolic behavior of *L. ferrooxidans*, thus, it could be used as a first approach to create new strategies to improve the productivity of the bioleaching processes.

Nomenclature

S	stoichiometric matrix
$v(x)$	vector of intracellular reaction rates
b	vector of extracellular reaction rates (substrate consumption and products formation) (mol/C-mol h^{-1})
q_{0_2}	specific oxygen consumption rate (mol O_2/C-mol h^{-1})
D	dilution rate (1/h)
r_i	generation rate of macromolecule i (mol i/C-mol h^{-1})
x_i	proportion of macromolecule i (mol/C-mol)
Y_{SX}	growth yield in substrate (ferrous iron) (C-mol/mol Fe^{2+})
q_S	specific substrate consumption rate (e.g., ferrous iron) (mol Fe^{2+}/C-mol h^{-1})
μ	specific growth rate (1/h)

We gratefully acknowledge the Millennium Scientific Initiative, Project ICM P05-001-F, for financial support of this work and CONICYT and BioSigma S.A. for support of M.P.M.

References

Bond PL, Banfield JF. 2001. Design and performance of rRNA targeted oligonucleotide probes for in situ detection and phylogenetic identification of microorganisms inhabiting acid mine drainage environments. Microb Ecol 41:116–149.

Boon M. 1996. Theoretical and experimental methods in the modeling of bio-oxidation kinetics of sulphide minerals. TU Dissertation, Delft: Department of Biochemical Engineering: Kluyiver Laboratory for Biotechnology, Delft University.

Boon M, Meeder TA, Thone C, Ras C, Heijnen JJ. 1999b. The ferrous iron oxidation kinetics of *Thiobacillus ferrooxidans* in continuous cultures. Appl Microbiol Biotechnol 51:820–826.

Boon M, Ras C, Heijnen JJ. 1999c. The ferrous iron oxidation kinetics of *Thiobacillus ferrooxidans* in batch cultures. Appl Microbiol Biotechnol 51:813–819.

Breed AW, Hansford GJ. 1999. Effect of pH on ferrous–iron oxidation kinetics of *Leptospirillum ferrooxidans* in continuous culture. Biochem Bioeng J 3:193–201.

Breed AW, Dempers CJN, Searby GE, Gardner MN, Rawlings DE, Hansford GJ. 1999. The effect of temperature on the continuous ferrous oxidation kinetics of a predominantly *Leptospirillum ferrooxidans* culture. Biotech Bioeng 65(1):44–53.

Edwards JS, Ibarra RU, Palsson BO. 2001. In silico predictions of *Escherichia coli* metabolic capabilities are consistent with experimental data. Nat Biotechnol 19(2):125–130.

Edwards JS, Covert M, Palsson BO. 2002. Metabolic modeling of microbes: The flux balance approach. Environ Microbiol 4(3):133–140.

Ferguson SJ, Ingledew WJ. 2008. Energetic problems faced by microorganisms growing or surviving on parsimonious energy sources and at acidic PH: I. *Acidithiobacillus ferrooxidans* as a paradigm. Biochem Biophys Acta 1777:1471–1479.

Hallberg KB, Lindström EB. 1994. Characterization of *Thiobacillus caldus* sp. nov., a moderately thermophilic acidophile. Microbiology 140: 3451–3456.

Hold C, Andrews B, Asenjo J. 2009. A stoichiometric model of *Acidithiobacillus ferrooxidans* ATCC 23270 for metabolic flux analysis. Biotech Bioeng 102(5):1448–1459.

Holmes D, Bonnefoy V. 2007. Genetic and bioinformatics insights into iron and sulfur oxidation mechanisms of bioleaching organisms. In: Rawlings D, Johnson B, editors. Biomining. Berlin, Hidelberg: Springer, p. 281–300.

Hügler M, Huber H, Stetter KO, Fuchs G. 2003. Autotrophic CO_2 fixation pathways in archaea (Crenarchaeota). Arch Microbiol 179:160–173.

Ingraham JL, Maaloe O, Neidhardt FC. 1983. Growth of the bacterial cell. Sunderland: Sinnauer Associates.

Jones CA, Kelly DP. 1983. Growth of *Thiobacillus ferrooxidans* on ferrous–iron in chemostat culture: Influence of product and substrate inhibition. J Chem Technol Biotechnol 33(4):241–261.

Kanamori K, Weiss R, Roberts J. 1987. Role of glutamate dehydrogenase in ammonia assimilation in nitrogen-fixing *Bacillus macerans*. J Bacteriol 169:4692–4695.

Kelly DP, Harrison AP. 1989. Genus *Thiobacillus* Beijerinck. In: Staley JT, Bryant MP, Pfennig N, Holt JG, editors. Bergey's manual of systematic bacteriology, Vol. 3. Baltimore: Williams & Wilkins, p. 1842–1858.

Kleerebezem R, Loosdrecht M. 2008. Thermodynamic and kinetic characterization using process dynamics: Acidophilic ferrous iron oxidation by *Leptospirillum ferrooxidans*. Biotechnol Bioeng 100(1):49–60.

Knorr A, Jain R, Srivastava R. 2007. Bayesian-based selection of metabolic objective functions. Bioinformatics 23(3):351–357.

Levican G, Bruscella P, Guacunano M, Inostroza C, Bonnefoy V, Holmes D, Jedlicki E. 2002. Characterization of the petI and res operons of *Acidithiobacillus ferrooxidans*. J Bacteriol 184:1498–1501.

Levican G, Ugalde J, Ehrenfeld N, Maass A, Parada P. 2008. Comparative genomic analysis of carbon and nitrogen assimilation mechanisms in three indigenous bioleaching bacteria: Predictions and validations. BMC Genome 9:581.

Menon S, Ragsdale SW. 1999. The role of iron–sulfur cluster in an enzymatic methylation reaction. J Biol Chem 274(17):11513–11518.

Mignone C, Donati E. 2004. ATP requirements for growth and maintenance of iron-oxidizing bacteria. Biochem Eng J 18:211–216.

Nielsen J, Villadsen J, Lidén G. 2003. Bioreaction engineering principles. New York: Kluw Acad Publ.

Norris PR, Murrel JC, Hinson D. 1995. The potential for diazotrophy in iron- and sulfur-oxidizing acidophilic bacteria. Arch Microbiol 164: 294–300.

Norris PR, Barr DW, Hinson D. 1998. Iron and mineral oxidation by acidophilic bacteria: Affinities for iron and attachment to pyrite. In: Norris PR, Kelly DP, editors. Biohydrometallurgy, Proceedings of the International Symposium 1987. Warwick: Science and Technology Letters, Kew., p. 43–60.

Okibe N, Gericke M, Hallberg KB, Johnson DB. 2003. Enumeration and characterization of acidophilic microorganisms isolated from a pilot plant stirred-tank bioleaching operation. Appl Environ Microbiol 69(4):1936–1943.

Oliveira AP, Nielsen J, Forster J. 2005. Modeling *Lactococcus lactis* using a genome-scale flux model. BMC Microbiol 5:39.

Olson GJ, Brierley JA, Brierley CL. 2003. Bioleaching review part B: Progress in bioleaching: applications of microbial processes by the mineral industries. Appl Microbiol Biotechnol 63:249–257.

Parro V, Moreno-Paz M. 2004. Nitrogen fixation in acidophile iron oxidizing bacteria: The nif regulon of *Leptospirillum ferrooxidans*. Res Microbiol 155:703–709.

Parro V, Moreno-Paz M, Gonzalez-Toril E. 2007. Analysis of environmental transcriptomes by DNA microarrays. Environ Microbiol 9: 453–464.

Rawlings DE. 1995. Restriction enzyme analysis of 16S rRNA genes for the rapid identification of *Thiobacillus ferrooxidans*, *Thiobacillus thiooxidans*, and *Leptospirillum ferrooxidans* strains in leaching environments. In: Jerez CA, Vargas T, Toledo H, Wiertz JV, editors. Biohydrometallurgical processing. Santiago: University of Chile, p. 9–17.

Rawlings DE. 2002. Heavy metal mining using microbes. Annu Rev Microbiol 56:65–91.

Rawlings DE. 2005. Characteristics and adaptability of iron- and sulfur-oxidizing microorganisms used for the recovery of metals from minerals and their concentrates. Microb Cell Fact 4:13.

Rawlings DE, Tributsch H, Hansford GS. 1999. Reasons why '*Leptospirillum*' – like species rather than *Thiobacillus ferrooxidans* are the dominant iron-oxidizing bacteria in many commercial processes for the biooxidation of pyrite and relates ores. Microbiology 145:5–13.

Roels JA. 1983. Energetics and kinetics in biotechnology. Amsterdam: Elsevier Biomedical Press.

Rohwerder T, Gehrke T, Kinzler K, Sand W. 2003. Bioleaching review part A: Progress in bioleaching: fundamentals and mechanisms of bacterial metal sulfide oxidation. Appl Microbiol Biotechnol 63:239–248.

Sand W, Rohde K, Sobotke B, Zenneck C. 1992. Evaluation of *Leptospirillum ferrooxidans* for leaching. Appl Environ Microbiol 58(1):85–92.

Savinell JM, Palsson BO. 1992a. Network analysis of intermediary metabolism using linear optimization. I. Development of mathematical formalism. J Theor Biol 154:421–454.

Savinell JM, Palsson BO. 1992b. Optimal selection of metabolic fluxes for *in vivo* measurements. I. Development of mathematical methods. J Theor Biol 155:201–214.

Scherpenzeel DAv, Boon M, Ras C, Handsford GS, Heijnen JJ. 1998. Kinetics of ferrous iron oxidation by *Leptospirillum* bacteria in continuous culture. Biotechnol Prog 14:425–433.

Schippers A, Sand W. 1998. Bacterial leaching of metal sulfides proceeds by two indirect mechanisms via thiosulfate or via polysulfides and sulfur. Appl Environ Microbiol 65:319–321.

Schrenk MO, Edwards KJ, Goodman RM, Hamers RJ, Banfield JF. 1998. Distribution of *Thiobacillus ferrooxidans* and *Leptospirillum ferrooxidans*: Implications for generation of acid mine drainage. Science 279:1519–1522.

Schuetz R, Kuepfer L, Sauer U. 2007. Systematic evaluation of objective functions for predicting intracellular fluxes in *Escherichia coli*. Mol Sysr Biol 3:1–15. (Article 119).

Silverman MP, Lundgren DG. 1959. Studies on the chemoautotrophic iron bacterium *Ferrobacillus ferrooxidans*. I: An improved medium and a harvesting procedure for securing high cell yields. J Bacteriol 77:642–647.

Stephanopoulos GN, Aristidou AA, Nielsen J. 1998. Metabolic engineering. London: Acad Press.

Tjaden B, Plagens A, Dörr C, Siebers B, Hensel R. 2006. Phosphoenolpyruvate synthetase and pyruvate, phosphate dikinase of *Thermoproteus tenax*: Key pieces in the puzzle of archaeal carbohydrate metabolism. Mol Microbiol 60(2):287–298.

Tyson G, Chapman J, Hugenholtz P, Allen E, Ram R, Richardson P, Solovyev R, Rokhsar D, Banfield J. 2004. Community structure and metabolism through reconstruction of microbial genomes from the environment. Nature 428:37–43.

Tyson G, Lo I, Baker B, Allen E, Hugenholtz P, Banfield J. 2005. Genome-directed isolation of the key nitrogen fixer *Leptospirillum ferrodiazotrophum* sp. nov. from an acidophilic microbial community. Appl Environ Microbiol 71:6319–6324.

White D. 1995. The physiology and biochemistry of prokaryotes. New York: Oxford University Press.